QUALITATIVE COMPARISON BETWEEN TWO OPEN WATER CANAL MODELS

João Nabais [*,1] **Miguel Ayala Botto** [**,1]

[*] *Instituto Politécnico de Setúbal*
Escola Superior de Tecnologia de Setúbal,
Campus do IPS, Estefanilha 2910-761 Setúbal, Portugal
e-mail: joao.nabais@estsetubal.ips.pt
[**] *Instituto Superior Técnico, TU-Lisbon*
Department of Mechanical Engineering, IDMEC
Av. Rovisco Pais, 1049-001 Lisboa, Portugal
e-mail: AyalaBotto@ist.utl.pt

Abstract: In this paper a comparison is made between two different dynamic models of an experimental open water canal situated in Évora, Portugal. A qualitative analysis focuses on the capacity of each model to accommodate different types of boundary conditions and monitoring the canal, while accounting for nonuniform geometric characteristics and dynamic accuracy. Both models are derived from the well known Saint-Venant equations, resulting in a finite dimension discrete-time model, and a simplified infinite dimension continuous-time model, respectively. The finite dimension model is shown to be more appropriate to be used in a fault tolerant control framework.

Keywords: Open Water canals, Saint Venant Equations, Fault Tolerant Control, Modeling, Time Delay Systems

1. INTRODUCTION

Water is a vital resource for earth biodiversity but is also essential for human kind way of life as it is used for industrial, domestic and agricultural purposes. In respect to Portugal, 81.8% of the available water is used for irrigation purposes (Raposo, 1996). In a near future UNESCO predicts that two out of three individuals will be affected by the lack of fresh water. The efficiency of water consumption is primordial for a sustainable development in the future.

Many of the currently existing water distribution networks are still manually operated. Only a few have monitoring equipment to support human decision, like for instance the SCADA system – Supervisory Control and Data Acquisition. To improve the efficiency on water use it is necessary to incorporate modern automatic control systems which are able to account for water flow deviations at some point in the water network (Silva *et al.*, 2007). Usually, water canals interact with end users through their physical offtakes. For simplicity and economic purposes in most of the irrigation systems water is supplied by gravity. The problem of supplying a given discharge is converted into controlling the water level at the offtake location. As the canal is constituted by several pools separated by gates, the offtake is normally immediately upstream the gate with a level sensor associated.

A typical open water canal is usually divided into several pools whose dynamics can be represented by the Saint Venant equations (Szymkiewicz, 2010), that is partial differential equation (PDE) of hyperbolic type. Hydraulic structures along the canal, like gates for instance, can also be modeled by a static relationship between upstream, downstream water levels

[1] This work is co-sponsored by project PTDC/EEA-CRO/102102/2008, FCT, Portugal.

and gates position. Through the separated implementation of all components it is possible to simulate a given open water canal using this type of models. The established model strategy proposed by (Litrico and Fromion, 2009) makes use of the Saint Venant equations to obtain an infinite dimension model described as an Input-Output transfer function. This type of model is specially suitable to frequency analysis but do require a high degree of complexity which limits their application to real time model based algorithms. On the other hand, the substantial simplified version of these models called the Integrator Delay Zero model (IDZ) (Litrico and Fromion, 2004) is suitable to real time applications but the simplifications used can only capture the main low and high frequency nature of the process.

This paper presents a qualitative study between the above mentioned two types of open water canal models. The purpose of this study is to be able to conclude which of these models is best suited to be used in a fault tolerant control strategy (Blanke *et al.*, 2006). Fault tolerant control as long proved to be a robust control technique to deal with complex systems subject to faults and disturbances, like an open water distribution canal. A key point to the success of this control strategy depends on the model accuracy and flexibility to incorporate faulty situations. A model that can be easy expanded to extract information along the canal is preferable to one that uses only upstream and downstream information. Also the possibility to use models that can easily monitor the canal behavior in different point locations is determinant to fault detection.

This paper has the following structure. Section 2 introduces the experimental water canal used in this study. In Section 3 two different types of dynamic models based on the linearized Saint Venant equations are presented for the water canal: a finite dimension discrete-time model, and an infinite dimension continuous-time one. In Section 4 the frequency and time responses of both models are compared in a simulation study. Finally, in Section 5 some conclusions are drawn.

2. EXPERIMENTAL WATER CANAL

The experimental water canal is located in Évora, Portugal, has 4 pools with a trapezoidal cross section of 900 mm height, 150 mm base width and a side slope of $m = 150$ mm. The distinct geometric characteristics for each pool are shown in Table 1. The 4 pools are divided by three sluice gates. All theses sluice gates are electro-actuated and instrumented with position sensors. A rectanguar overshot gate is located at the end of the canal with 700 mm width. The off-take valves, equipped with an electromagnetic flow-meter and motorized butterfly valve for flow control, are immediately located upstream of each sluice gate. Counterweight-float level sensors are distributed along the canal, as shown in Fig. 1.

Table 1. Geometric characteristics

	Total length – L [m]	Slope – I
Pool 1	40.37	0.0016
Pool 2	34.87	0.0014
Pool 3	35.14	0.0019
Pool 4	26.55	0.0004

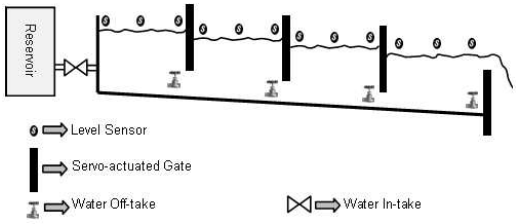

Fig. 1. Schematics of the complete facility

At the head of the canal an electro-valve controls the canal inflow. This flow is extracted from a reservoir as depicted in figure 1. The maximum flow capacity is 0.090 m^3/s. The water canal nominal capacity provides a flow of 0.030 m^3/s for a uniform water depth of 0.600 m. All electro-actuators and sensors in the canal are connected to local PLCs (Programmable Logic Controllers) responsible for the sensor data acquisition and for the control actions sent to the actuators. All local PLCs are connected through a MODBUS network (RS 485) (Figueiredo and Ayala Botto, 2005).

3. MATHEMATICAL MODEL

3.1 *Saint Venant Equations*

The mathematical model of the water canal will be derived based on first principles physical relations to an hydraulic control volume (Sabersky *et al.*, 1998).

The derived set of equations is known as the Saint-Venant equations,

$$\frac{\partial Q(x,t)}{\partial x} + B(x,t)\frac{\partial Y(x,t)}{\partial t} = 0 \qquad (1)$$

$$\frac{\partial Q(x,t)}{\partial t} + \frac{\partial}{\partial x}\left(\frac{Q^2(x,t)}{A(x,t)}\right) + \ldots$$
$$\ldots + g \cdot A(x,t) \cdot (J(x,t) - I(x)) = 0 \qquad (2)$$

where $Q(x,t)$ is the discharge, $Y(x,t)$ the water surface level, $B(x,t)$ the water surface width, $A(x,t)$ the water cross-section area, g the gravity acceleration, x the longitudinal abscissa in the flow direction, t the time instant, $I(x)$ the bottom slope and $J(x,t)$ the energy gradient slope that can be accurately approximated by the following Manning-Strickler empirical formula (Quintela, 2005),

$$J(x,t) = \frac{P(x,t)^{4/3}}{K^2 A(x,t)^{10/3}} Q(x,t)\,|Q(x,t)| \qquad (3)$$

where K is the Manning-Strickler coefficient (determined to be 65 $m^{1/3}/s$) and $P(x,t)$ is the wetted perimeter. These equations are non-linear with unknown analytical solution.

The flow type on open water is classified according to the Froude number, that can be seen as the ratio between inertial and gravity forces,

$$F_r(x,t) = V(x,t)\sqrt{\frac{B(x,t)}{g \cdot A(x,t)}} = \frac{V(x,t)}{C(x,t)} \quad (4)$$

where, $C(x,t) = \sqrt{g\frac{A(x,t)}{B(x,t)}}$, is the wave celerity. In this work only subcritical flow is considered, that is to say $F_r < 1$.

For control purposes it is recommended to work around a steady state with a linear model. To accomplish this the Saint Venant equations are first linearized around an equilibrium point and only then discretized.

3.2 *Linearized Saint Venant Equations*

Consider a steady state defined as $(Q_0, Y_0(x))$ where index 0 stands for steady point configuration. The deviation variables are defined as,

$$\begin{aligned} q(x,t) &= Q(x,t) - Q_0 \\ y(x,t) &= Y(x,t) - Y_0(x) \end{aligned}$$

Assuming $A(x,t) = B_0(x)Y(x,t)$, after linearization equations (1) (2) become,

$$B_0(x)\frac{\partial y(x,t)}{\partial t} + \frac{\partial q(x,t)}{\partial x} = 0 \quad (5)$$

$$\frac{\partial q(x,t)}{\partial t} + 2V_0(x)\frac{\partial q(x,t)}{\partial x} + \delta(x)q(x,t) + \ldots + \left[C_0^2(x) - V_0^2(x)\right] B_0(x)\frac{\partial y(x,t)}{\partial x} - \tilde{\gamma}(x)y(x,t) = 0 \quad (6)$$

where,

$$\begin{aligned} C_0(x) &= \sqrt{g\frac{A_0(x)}{B_0(x)}} \\ \alpha(x) &= C_0(x) - V_0(x) \\ \beta(x) &= C_0(x) - V_0(x) \\ \delta(x) &= \frac{2 \cdot g}{V_0(x)}\left(J_0(x) - Fr_0^2(x)\frac{dY_0(x)}{dx}\right) \\ Fr_0^2(x) &= \frac{V_0^2(x)B_0(x)}{g \cdot A_0(x)} \\ \tilde{\gamma}(x) &= V_0^2(x)\frac{dB_0(x)}{dx} + g \cdot B_0(x)\left[D(x)J_0(x) + \ldots \right. \\ &\quad \left. + I(x) - \left(1 + 2Fr_0^2(x)\right)\frac{dY_0(x)}{dx}\right] \\ D(x) &= \frac{7}{3} - \frac{4}{3}\frac{A_0(x)}{P_0(x)B_0(x)}\frac{\partial P_0(x)}{\partial y} \end{aligned} \quad (7)$$

To complete the linearized pool model is necessary to consider an initial condition along the spatial coordinate,

$$q(x,0) = q_0(x) \qquad y(x,0) = y_0(x) \quad (8)$$

and two boundary conditions on each end along time,

$$q(0,t) = u_1(t) \qquad q(L,t) = u_2(t) \quad (9)$$

To simplify future analysis the Saint Venant equations can be written to a more convenient alternative form. For that consider the area deviation as $a(x,t) = B_0(x)y(x,t)$. The linearized equations (5) and (6) are now,

$$\frac{\partial a(x,t)}{\partial t} + \frac{\partial q(x,t)}{\partial x} = 0 \quad (10)$$

$$\frac{\partial q(x,t)}{\partial t} + \left[\alpha(x) - \beta(x)\right]\frac{\partial q(x,t)}{\partial x} + \ldots + \alpha(x)\beta(x)\frac{\partial a(x,t)}{\partial x} + \delta(x)q(x,t) - \gamma(x)a(x,t) = 0 \quad (11)$$

where,

$$\gamma(x) = \frac{C_0^2(x)}{B_0(x)}\frac{dB_0(x)}{dx} + g\left[\left(1 + D(x)\right)I(x) + \ldots - \left(1 + D(x) - (D(x) - 2)Fr_0^2(x)\right)\frac{dY_0(x)}{dx}\right] \quad (12)$$

Considering the state vector $\chi(x,t) = \begin{bmatrix} q(x,t) & a(x,t) \end{bmatrix}'$ equations (10) and (11) may be expressed in state space,

$$A\frac{\partial}{\partial t}\chi(x,t) + B(x)\frac{\partial}{\partial x}\chi(x,t) + C(x)\chi(x,t) = 0 \quad (13)$$

where,

$$A = \begin{bmatrix} 0 & 1 \\ 1 & 0 \end{bmatrix} \qquad B(x) = \begin{bmatrix} 1 & 0 \\ \alpha(x) - \beta(x) & \alpha(x)\beta(x) \end{bmatrix}$$

$$C(x) = \begin{bmatrix} 0 & 0 \\ \delta(x) & -\gamma(x) \end{bmatrix}$$

3.3 *Continuous Models*

From (13) after laborious mathematical manipulations a continuous multivariable model, input–output transfer matrix, relating upstream and downstream water level to upstream and downstream discharge, has been developed (Litrico and Fromion, 2009),

$$\begin{bmatrix} y(0,s) \\ y(L,s) \end{bmatrix} = \begin{bmatrix} p_{11}(s) & p_{12}(s) \\ p_{21}(s) & p_{22}(s) \end{bmatrix}\begin{bmatrix} q(0,s) \\ q(L,s) \end{bmatrix} \quad (14)$$

The input–output transfer matrix is specially suited for properties analysis and frequency analysis supporting H_∞ design. Although accurate these models

are too complex and may compromise real time implementations. From this structure a simplified model named Integral Delay Zero is available (Litrico and Fromion, 2004).

The IDZ model is valid for the uniform and nonuniform flow conditions and captures the main physical properties of open canal dynamics. The model is accurate for the most important dynamic characteristics as the integrator gain and time delay. The zero accounts for direct influence of discharge on the water level for high frequency. The model has only a few parameters, the integrator gain, the time delay and zeros, which can be computed analytically from the steady state configuration. The model is structurally identical to (14) only with different elements $p_{ij}(s)$ calculated by,

$$
\begin{aligned}
p_{11}(s) &= \frac{1}{A_u s} + \tilde{b}_u \\
p_{12}(s) &= -\left(\frac{1}{A_u s} + b_u\right) e^{-\tau_1 s} \\
p_{21}(s) &= \left(\frac{1}{A_d s} + b_d\right) e^{-\tau_2 s} \\
p_{22}(s) &= -\frac{1}{A_d s} + \tilde{b}_d
\end{aligned}
$$

The transfer function $p_{21}(s)$ describes the effect of upstream discharge to downstream water depth. The time delay τ_1 represents the time for a change in the upstream discharge to produce an effect on the downstream water depth. Transfer function $p_{12}(s)$ describes the effect of a change in the downstream discharge to have effect in the upstream water depth. Interpretation of τ_2 is analogous to τ_1. For uniform flow the time delays are calculated by $\tau_1 = L/\alpha = L/(V_0 + C_0)$ and $\tau_2 = L/\beta = L/(C_0 - V_0)$. A canal pool can be divided into two parts; the uniform part located upstream where the water depth is approximately constant, and a nonuniform part located at the downstream end where the water level is slow moving with an approximately horizontal surface caused by a flow obstruction as a gate. The integrator constants A_u and A_d correspond to the superficial area for uniform and nonuniform flows respectively. The constants b_i are related to high frequency gain.

3.4 *Discrete Models*

The Saint Venant discretization is done over a grid of spaced lines, horizontal for time and vertical for space, Fig. 2, where, Δx is the spatial mesh dimension, Δt is the time step, θ and ϕ weighting parameters ranging from 0 to 1, k is time level index and i is cross-section index. A function value and its partial derivatives inside a grid square are calculated from the square node values accordingly to (15)–(17).

$$
f(x,t) = \theta\left[\phi f_{i+1}^{k+1} + (1-\phi) f_i^{k+1}\right] + (1-\theta)\left[\phi f_{i+1}^{k} + (1-\phi) f_i^{k}\right] \tag{15}
$$

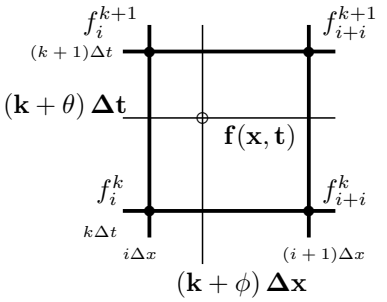

Fig. 2. Interpolation using the *Box Scheme*.

$$
\frac{\partial f}{\partial x}(x,t) = \theta\frac{f_{i+1}^{k+1} - f_i^{k+1}}{\Delta x} + (1-\theta)\frac{f_{i+1}^{k} - f_i^{k}}{\Delta x} \tag{16}
$$

$$
\frac{\partial f}{\partial t}(x,t) = \phi\frac{f_{i+1}^{k+1} - f_{i+1}^{k}}{\Delta t} + (1-\phi)\frac{f_{i}^{k+1} - f_{i}^{k}}{\Delta t} \tag{17}
$$

For $\phi = 0.5$ it correspond to the Preissmann method. Changing θ means moving the evaluation point in time. The state vector for two consecutive sections is fourth dimension with both upstream and downstream discharge and area deviation, $x(k) = \left[\, q_i^k \;\; a_i^k \;\; q_{i+1}^k \;\; a_{i+1}^k \,\right]^T$. Applying (15)–(17) to equation (13) after some manipulations we get the discrete state space system,

$$
\begin{bmatrix} a_{11} & a_{21} \\ a_{12} & a_{22} \\ a_{13} & a_{23} \\ a_{14} & a_{24} \end{bmatrix}^T \begin{bmatrix} q_i^{k+1} \\ a_i^{k+1} \\ q_{i+1}^{k+1} \\ a_{i+1}^{k+1} \end{bmatrix} + \begin{bmatrix} b_{11} & b_{21} \\ b_{12} & b_{22} \\ b_{13} & b_{23} \\ b_{14} & b_{24} \end{bmatrix}^T \begin{bmatrix} q_i^{k} \\ a_i^{k} \\ q_{i+1}^{k} \\ a_{i+1}^{k} \end{bmatrix} = 0 \tag{18}
$$

The state space representation describes the pool dynamics between two adjacent sections. To obtain the model corresponding to a pool divided into n section it is necessary to use $n+1$ sections leading to $2(n+1)$ variables. Using model (18) is possible to obtain $2n$ equations. The last two equations are related to the upstream and downstream boundary conditions. The total pool state vector $\mathbf{X}(k)$ is defined as,

$$
\begin{aligned}
\mathbf{X}(k) = \big[\, & q_1(k) \;\; a_1(k) \;\; q_2(k) \;\; a_2(k) \;\; \ldots \\
& \ldots \; q_n(k) \;\; a_n(k) \;\; q_{n+1}(k) \;\; a_{n+1}(k) \,\big]
\end{aligned} \tag{19}
$$

The final reach model is represented in state space by,

$$
\begin{aligned}
\mathbf{X}(k+1) &= A_k \mathbf{X}(k) + B_k \mathbf{u}(k) \\
\mathbf{Y}(k) &= C_k \mathbf{X}(k)
\end{aligned} \tag{20}
$$

Matrices A_k and B_k are square sparse matrix with dimension $2(n+1)$, matrix B_k has dimension $2(n+1)\times 2$ to account for both boundary conditions and matrix C_k has variable dimension according to the outputs used. The model will be naturally dependent on the discretization parameters used, specifically θ and Δt. Understanding the physical process and discretization technique is vital to identify unphysical behavior in the solution (Szymkiewicz, 2010).

Table 2. Dynamical parameters

	Pool 1	Pool 2	Pool 3	Pool 4
$C_0(L)$	2.0690	2.0690	2.0690	2.0690
$\alpha(L)$	2.2773	2.2773	2.2773	2.2773
$\beta(L)$	1.8607	1.8607	1.8607	1.8607
$\delta(L)$	0.0180	0.0182	0.0177	0.0192
$\gamma(L)$	0.0101	0.0093	0.0112	0.0057
$F_{r_0}(L)$	0.0101	0.0101	0.0101	0.0101
$D(L)$	1.4703	1.4703	1.4703	1.4703

Table 3. IDZ parameters

	A_u	A_d	τ_1	τ_2
pool 1	13.39	12.78	18.09	22.55
pool 2	11.56	11.11	15.55	19.23
pool 3	11.46	11.02	15.56	19.42
pool 4	11.82	11.34	15.48	18.99

	$\tilde{b}_u$	b_u	b_d	$\tilde{b}_d$
pool 1	1.534	1.956	2.048	1.591
pool 2	1.517	1.960	2.039	1.567
pool 3	1.541	1.998	2.077	1.591
pool 4	1.471	1.886	1.966	1.520

4. SIMULATION RESULTS

4.1 *The experimental water canal data*

The spacial step was considered equal to $L/10$. The water level elevation for steady state can be computed numerically from the relation,

$$\frac{dY(x)}{dx} = \frac{I - J(x)}{1 - \frac{V_0^2(x)B_0}{gA_0(x)}} \tag{21}$$

The dynamical parameters (7) and (12) along the canal axis are indicated in Table 2.

Output matrix C_k in (20) will be defined to produce a model similar do the IDZ model, relating the upstream and downstream discharge deviations to upstream and downstream water level deviations. C_k is responsible to convert the water area deviation in state vector (19) to water level deviation. In Table 3 the IDZ model parameters are presented for all pools. For the nonuniform case the Input-Output matrix (Litrico and Fromion, 2009) poles can be asymptotically approximated. Table 4 indicates the asymptotic frequency values of the canal poles. The models presented here

Table 4. Asymptotic natural frequency

	Pool 1	Pool 2	Pool 3	Pool 4
$k_p = \pm 1$	0.1549	0.1811	0.1798	0.1826
$k_p = \pm 2$	0.3094	0.3619	0.3593	0.3648
$k_p = \pm 3$	0.4639	0.5427	0.5388	0.5470
$k_p = \pm 4$	0.6185	0.7236	0.7184	0.7293
$k_p = \pm 10$	1.5461	1.8088	1.7959	1.8232

were implemented and tested in Simulink.

4.2 *Calibrating Finite Dimension Model*

Passing from an infinite model to a finite one implies some inaccuracies. In fact the finite dimension model performance will be a function of parameters Δx, Δt, and θ. The spatial grid mesh dimension was fixed to $\frac{L_i}{10}$ which is a common value for open water canal as a compromise between accuracy and computational complexity. Here the centered scheme, $\theta = 0.5$, was implemented which is second order accurate and unconditionally stable for $\theta \geq 0.5$. The time step can be adjusted to improve model performance. As an initial guess we may expect that reducing time step will improve the model. Consider the Courant number defined,

$$C_r = \frac{\alpha \Delta t}{\Delta x} \tag{22}$$

A natural frequency error analysis depending on Courant number was performed. The error is minimal for three different Courant number: $C_r = 0.9$ minimizes the error for ω_1, $C_r = 1.1$ minimizes the error for ω_2 while the higher frequencies error is minimized for $C_r = 1.14$. The same analysis for pools 2 to 4 give similar results. In Fig. 3 the three different configurations for C_r are tested for pool 1 with a positive step input at downstream end. Physically this is equivalent to operate a pump at downstream end, this will diminish the water level. Simultaneously a wave will travel from downstream to upstream end with an immediate effect in water level. From Fig. 3(a) and 3(b) is possible to see how the wave is propagated along the canal axis. A higher Courant number, that is to say a higher time step, reduces significantly the unphysical oscillations introduced numerically. At the same time the diffusion is also reduced as the front wave persists until the upstream end. In Fig. 3(c) and 3(d) the higher Courant number configuration has a more smooth response with some discontinuities corresponding to the first oscillating mode, the time required for a wave to travel both ways, $\tau_1 + \tau_2 \simeq 40$s. Naturally the best

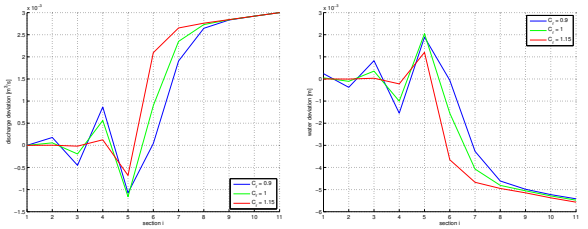

(a) Discharge deviation profile for $t = 6 \times \Delta t$s.

(b) Water deviation profile for $t = 6 \times \Delta t$s.

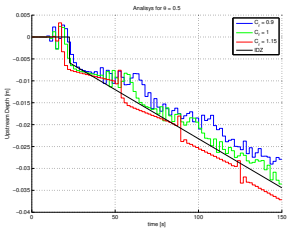

(c) Upstream water level.

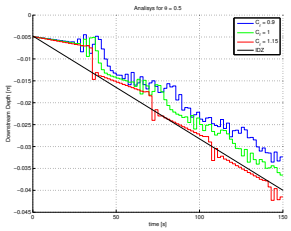

(d) Downstream water level.

Fig. 3. Pool 1 behavior for a downstream step input of magnitude $0.1Q_0$.

Table 5. Natural frequency error between asymptotic and Saint Venant poles

Pool	1 [%]	2 [%]	3 [%]	4 [%]
$k_p = \pm 1$	0.12	0.05	0.08	0.03
$k_p = \pm 2$	0.61	0.64	0.62	0.68
$k_p = \pm 3$	1.67	1.64	1.68	1.57
$k_p = \pm 4$	3.06	2.96	3.08	2.74
$k_p = \pm 10$	13.69	13.01	13.82	11.48

numerically configuration for representing the Évora canal is $\theta = 0.5$ and $C_r = 1.15$.

4.3 *Model Verification*

For the established discretization configuration in Table 5 the natural frequency error for some poles is presented. As can be seen the error is insignificant for the first pairs. In Fig. 4 the magnitude frequency response is indicated. To access the interaction between

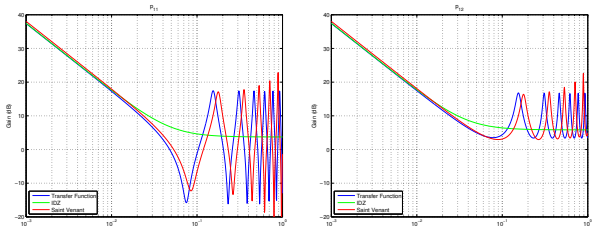

(a) $q(0,\omega)$ to $y(0,\omega)$.

(b) $q(L,\omega)$ to $y(0,\omega)$.

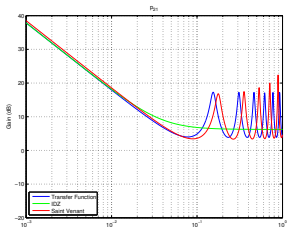

(c) $q(0,\omega)$ to $y(L,\omega)$.

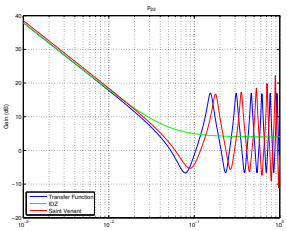

(d) $q(L,\omega)$ to $y(0,\omega)$.

Fig. 4. Magnitude frequency response for Pool 4.

each pool model and hydraulic structures the experimental water canal will be considered in one of its possible configurations: pool 4 with an overshot gate at downstream. Fig. 5 presents the simulation results for a step input $0.1 \times Q_0$ in upstream discharge variation. The downstream water level deviation is similar between finite and infinite models. The finite model configuration proposed is the one with less oscillations at downstream water level before wave arrival. The undershoot presented by the other finite models is eliminated and transformed into an overshot. At the upstream water level some differences are significant. The infinite model has a different final value. There is a significant discontinuity corresponding to wave propagation time from downstream to upstream. This can have an undesired effect when a hydraulic structure is connected to the upstream end of a pool. If the gate is of undershot type it will propagate the discontinuity into the upstream pools.

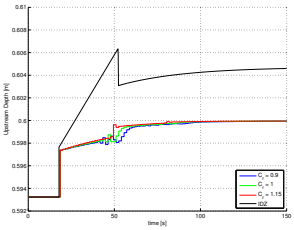

(a) Upstream water deviation.

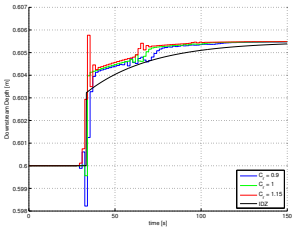

(b) Downstream water deviation.

Fig. 5. Time response for an upstream step input of $0.1 \times Q_0$ for pool 4 with an overshoot gate.

5. CONCLUSIONS

This paper presents a comparison between two different types of dynamic models of an open water canal: an infinite dimension and a finite dimension one. The infinite model is best suited for frequency design while the finite model is more adequate for time design. While the infinite dimension model suffers from a lack of capacity for monitoring the canal, as only the upstream and downstream water deviations are available, the finite dimension model allows for a better supervision of both water and discharge deviation along the canal axis. Thus, the finite dimension model can accommodate sensorial capacity along the canal, which makes it more suitable to be used in fault tolerant control schemes.

6. REFERENCES

Blanke, Mogens, Michel Kinnaert, Jan Lunze and Marcel Staroswiecki (2006). *Diagnosis and Fault-Tolerant Control*. 2nd ed.. Springer-Verlag. Berlin.

Figueiredo, J. and M. Ayala Botto (2005). Automatic control strategies implemented on a water canal prototype. In: *Proceedings of 16th IFCA World Congress*. Praha, Czech Republic.

Litrico, Xavier and Vincent Fromion (2004). Simplified modeling of irrigation canals for controller design. *Journal of Irrigation and Drainage Engineering* pp. 373–383.

Litrico, Xavier and Vincent Fromion (2009). *Modeling and Control of Hydrosystems*. Springer-Verlag. London.

Quintela, A. C. (2005). *Hidráulica*. 9th ed.. Fundação Calouste Gulbenkian.

Raposo, J. R. (1996). *A Rega: dos primitivos regadios às modernas técnicas de rega*. 1st ed.. Fundação Calouste Gulbenkian.

Sabersky, R. H., A. J. Acosta, E. G. Hauptmann and E. M. Gates (1998). *Fluid Flow: A First Course in Fluid Mechanics*. 4th ed.. Prentice Hall.

Silva, Pedro, Miguel Ayala Botto and João Figueiredo (2007). Model predictive control of an experimental water canal. In: *European Control Conference*. Kos, Grécia. pp. 2977–2984.

Szymkiewicz, Romuald (2010). *Numerical Modeling in Open Channel Hydraulics*. Springer-Verlag.